



Insights into uncertainties in future drought analysis using hydrological simulation model

Jin Hyuck Kim¹, Eun-Sung Chung^{2*}

¹ Department of Civil Engineering, Chungnam National University, 99 Daehak-ro, Yuseong-gu, Daejeon 34134, South Korea.

² Faculty of Civil Engineering, Seoul National University of Science and Technology, 232 Gongneung-ro, Nowon-gu, Seoul 01811, South Korea.

*Corresponding author (eschung@seoultech.ac.kr)

Abstract

Hydrological analysis utilizing a hydrological model requires a parameter calibration process, which is largely influenced by the length of calibration data period and prevailing hydrological conditions. This study aimed to quantify these uncertainties in future runoff projection and hydrological drought based on future climate data and the calibration data of the hydrological model. Future climate data were sourced from three Shared Socioeconomic Pathway (SSP) scenarios (SSP2-4.5, SSP3-7.0, and SSP5-8.5) of 20 general circulation models (GCMs). The Soil and Water Assessment Tool (SWAT) was employed as the hydrological model, and hydrological conditions were determined using the Streamflow Drought Index (SDI), with calibration data lengths ranging from 1 to 20 years considered. Subsequently, the uncertainty was quantified using Analysis of Variance (ANOVA). After calibrating the SWAT parameters, the validation performance was found to be influenced by the hydrological conditions of the calibration data. Hydrological model parameters calibrated using a dry period simulated runoff with 11.4% higher performance in dry conditions and 6.1% higher performance in normal conditions, while hydrological model parameters calibrated using a wet period simulated runoff with 5.1% higher performance in wet conditions. The uncertainty contribution of the hydrological model in estimating future runoff was analyzed to be 3.9~9.8%, particularly significant in the low runoff period. The uncertainty contribution in future hydrological drought analysis resulting from the calibration of hydrological model parameters was analyzed to be 2.7% on average, which is lower than that of future runoff projection.

Key words: Future runoff, Hydrological drought, GCM, SWAT, Uncertainty



36 **1. Introduction**

37 In the current global climate scenarios, characterized by significant warming trends, there are
38 increased challenges in understanding and managing water systems (IPCC, 2014; IPCC, 2021).
39 Water availability for runoff is directly influenced by precipitation, while temperature affects
40 water availability through its effect on evapotranspiration rates (Mahabadi and Delavar, 2024).
41 These climatic changes significantly affect the availability of water resources and increase the
42 occurrence and severity of hydrological extreme events such as floods and droughts in different
43 regions (Milly et al., 2008; Santos et al., 2021). Hydrological projection is crucial for
44 sustainable water resource planning and management (Peng et al., 2022; Yang et al., 2023;
45 Yang et al., 2024). Consequently, quantifying the uncertainty in hydrological projection is
46 essential as it directly affects the effectiveness of these management strategies and decision-
47 making processes in ensuring the reliability and safety of water resources (Zhang et al., 2024).

48 Droughts, which could become more severe due to climate change, begin with a lack of
49 precipitation and lead to a decrease in streamflow and soil moisture deficiency, encompassing
50 a complex hydrological cycle that adversely affects plant and crop growth and human life.
51 Generally, droughts progress over time into meteorological, agricultural, hydrological, and
52 socio-economic droughts, and become a fatal disaster if prolonged (Sheffield and Wood, 2012).
53 Consequently, future droughts due to climate change has been actively conducted, with most
54 studies concluding that droughts are becoming more frequent and severe (Sung et al., 2018;
55 Kim et al., 2021).

56 Hydrological drought requires an understanding of the hydrological cycle, including runoff,
57 surface water, and groundwater. Runoff, a key indicator of hydrological drought, significantly
58 affects the availability of water for agricultural, industrial, and domestic uses (Ghasemizade
59 and Schirmer, 2013; Devia et al., 2015). Therefore, understanding and predicting runoff
60 behavior is essential for hydrological drought analysis in water resource management and
61 planning. While runoff data can be obtained from river observations within the region, there
62 are limitations in observation technology and coverage. Consequently, simulated runoff data
63 using regional meteorological data and hydrological models are utilized. Hydrological models
64 simulate runoff by inputting meteorological data, soil data, and topographical data, allowing
65 for the prediction of future hydrological cycles. However, these hydrological models are
66 influenced by various factors, including the quality and quantity of input data, structural
67 uncertainties of the models, and uncertainties in the calibration process (Xu et al., 2007; Renard



68 et al., 2010). Therefore, quantifying and recognizing these uncertainties is crucial to enhancing
69 the reliability of future hydrological analysis (Feng et al., 2019).

70 The future hydrological analyses considering uncertainty is essential for effective water
71 management. These projections are largely based on General Circulation Models (GCMs) and
72 hydrological models, which are critical tools for modelling the hydrological impacts of climate
73 change. However, GCMs introduce significant uncertainty in future runoff prediction due to
74 their inherent structural complexity and variability in scenario-based inputs (Broderick et al.,
75 2016). This uncertainty has a direct impact on the accuracy of runoff predictions and poses a
76 significant challenge to water resource management. The selection and use of GCMs have a
77 crucial role in shaping these uncertainties, making the consideration of a variety of GCMs and
78 shared socioeconomic pathways (SSP) scenarios essential for managing uncertainties and
79 improving projections (Vetter et al., 2015; Chae et al., 2024a). Indeed, Shi et al. (2022) had
80 shown how different evapotranspiration models embedded in GCMs affect runoff prediction,
81 highlighting GCMs and Representative Concentration Pathways (RCPs) as major factors
82 affecting uncertainty. Similarly, Lee et al. (2021a) had shown how the choice of GCMs
83 significantly affects prediction of water storage in wetlands under future climate scenarios. To
84 understand these uncertainties, Wang et al. (2020) suggested the use of a broad ensemble of at
85 least 10 GCMs, which allowed for a more comprehensive assessment of hydrological impacts
86 and helped to reduce the inherent uncertainties associated with climate change. Thus, the use
87 of a wide range of GCMs is an essential strategy for maximizing the effectiveness of water
88 resource management under global climate change conditions.

89 The hydrological model calibration involves significant uncertainty, especially when
90 predicting future conditions. This process, crucial for aligning model parameters with historical
91 data, often incorrectly assumes that parameters validated under past hydrological conditions
92 will remain valid in the future. Thirel et al. (2015) and Fowler et al. (2016) demonstrated that
93 models calibrated with historical climate data might not perform accurately under changed
94 conditions, leading to substantial uncertainties in runoff projections. This challenge is
95 exacerbated by the dependency of model parameters on the hydrological conditions prevalent
96 during the calibration period (Merz et al., 2011; Coron et al., 2012). Effective calibration
97 strategies, therefore, must consider variable climate scenarios to ensure model robustness. This
98 involves rigorous calibration under diverse conditions to validate hydrological models'
99 reliability in projecting future water resource availability (Saft et al., 2016; Dakhlaoui et al.,
100 2017). Furthermore, the interaction between model parameters and hydrological conditions



101 during these periods often complicates the calibration process, underscoring the need for robust
102 validation techniques. The duration of the calibration period also contributes significantly to
103 the uncertainty in runoff projection. Razavi and Tolson (2013) and Arsenault et al. (2018)
104 highlighted the importance of sufficiently long calibration periods to ensure meaningful
105 calibration and validation results. In addition, Kim et al. (2011) cautioned against using overly
106 short calibration periods, as this can lead to large and unstable model performance variability
107 during calibration and validation. Despite the emphasis on longer calibration periods, Perrin et
108 al. (2007), Sun et al. (2017), Yu et al. (2023), and Ziarh et al. (2024) had found that an extended
109 calibration data length does not guarantee improved model performance, suggesting a nuanced
110 approach to calibration period selection. These insights underlined the complex interplay
111 among calibration length, model parameter selection, and climatic variability in shaping the
112 reliability of hydrological models.

113 The rigorous quantification of uncertainties in hydrological modeling is essential to enhance
114 the reliability of water resources planning and management. This study employs Analysis of
115 Variance (ANOVA), a statistical method widely used in hydrological studies, to systematically
116 quantify uncertainties in hydrological projections. ANOVA dissects the variance observed in
117 projections into contributions from various sources of uncertainty, such as GCM outputs, SSP
118 scenarios, and hydrological model parameters (Qi et al., 2016; Chae et al., 2024b). By
119 identifying the dominant sources of variability and analyzing their interactions, ANOVA
120 provides a clear understanding of how different factors drive uncertainties in hydrological
121 projections. Recent applications of ANOVA in future hydrological studies demonstrated its
122 effectiveness in understanding model-driven uncertainties (Chen et al., 2022; Yuan et al., 2022;
123 Mo et al., 2024).

124 This study focuses on the uncertainty in future hydrological analyses, which are influenced by
125 hydrological model parameters during different calibration periods under future climate data
126 and different hydrological conditions. This research utilizes the Soil and Water Assessment
127 Tool (SWAT), a widely recognized hydrological model, to analyze the impact of hydrological
128 conditions during the calibration period on the projection of future runoff and hydrological
129 drought. Three SSP scenarios and 20 GCMs were used to consider uncertainty due to future
130 climate, and different hydrological conditions according to the Streamflow Drought Index (SDI)
131 and different calibration period data lengths from 1 to 20 years were used to consider
132 uncertainty in hydrological model parameter calibration. This study aims to contribute to the



133 refinement of hydrological modelling practices by quantifying the uncertainties associated with
134 future runoff projection and hydrological drought analysis.

135 This manuscript is structured as follows. In Section 2, the study area, datasets, and the
136 methodologies used in this study are described, including the SWAT model, the ANOVA
137 framework, and the statistical validation procedures. In Section 3, the results of the analysis
138 are presented, showing the effects of calibration conditions on model performance and
139 quantifying the uncertainty contributions from various sources for both future runoff and
140 hydrological drought. In Section 4, the implications of these findings are discussed in the
141 context of previous research. Finally, Section 5 summarizes the main conclusions of this study.

142

143 **2. Methodology**

144 **2.1 Procedure**

145 The procedure of the study is as follows. First, topographic data for four dam basins in South
146 Korea were established, taking into account the overall hydrological characteristics of the
147 region, and observed dam inflow data were utilized to consider the length and hydrological
148 conditions of the hydrological model calibration data. The length of the calibration data
149 considered ranged from 1 to 20 years, and hydrological conditions were categorized using the
150 Streamflow Drought Index (SDI). Subsequently, validation performance analysis was
151 conducted, with calculations varying according to the length of calibration data and
152 hydrological conditions (Dry, Normal, and Wet). For the study, future climate data from 20
153 Coupled Model Intercomparison Project Phase 6 (CMIP6) GCMs and three SSP scenarios
154 (SSP2-4.5, SSP3-7.0, and SSP5-8.5) were bias-corrected. Future runoff projection and
155 hydrological drought were then analyzed using calibrated hydrological model parameters under
156 different conditions along with the future climate data. Finally, the uncertainties in the future
157 hydrological analysis were quantified using the Analysis of Variance (ANOVA).

158

159 **2.2 Study area and datasets**

160 The study areas selected in this study are the Andong (AD), Chungju (CJ), Habcheon (HC),
161 and Seomjingang (SJ) dam basins located in Korea as shown in Fig. 1. To achieve stable
162 calibration and validation results for a hydrological model, it is imperative to choose



catchments with extensive hydrological data records. This enables the accurate estimation of appropriate calibration data lengths through various testing periods of the hydrological model. Furthermore, incorporating a variety of basins is crucial to ensure that the findings of this study are not biased by specific hydrological conditions. These four basins, which have the longest hydrological records in Korea, are situated in major river basins as shown in Table S1: AD (1,584 km²) and HC (925 km²) in the southeastern Nakdong River basin, CJ (6,648 km²) in the southern Han River basin, and SJ (763 km²) in the southwestern Seomjin River basin. These regions are devoid of artificial structures, ensuring that runoff remains natural and unaltered. Located in different regions of Korea, these basins have a range of hydrological conditions and runoff characteristics, providing a representative cross-section of the country's hydrological characteristics.

2.3 Soil and water assessment tool (SWAT)

The SWAT was used to calibrate hydrological processes in our study basin. The SWAT is particularly adept at simulating runoff and other hydrological variables under a wide range of environmental conditions and is a robust, physically based, semi-distributed model. Its efficiency in modelling hydrological cycles within basins relies on simple input variables to produce detailed hydrological outputs. The capability of this model has been effectively shown in various studies, including those in South Korea (Kim et al., 2022; Song et al., 2022).

The core of the SWAT model is the water balance equation, which integrates daily weather data with land surface parameters to calculate water storage changes over time:

$$SW_t = SW_0 + \sum_{i=0}^t (R_{day} - Q_{surf} - E_a - w_{seep} - Q_{gw}) \quad (1)$$

where SW_0 is the initial soil moisture content (mm), SW_t is the total soil moisture per day (mm), R_{day} is precipitation (mm), Q_{surf} is surface runoff (mm), E_a is evapotranspiration (mm), W_{seed} is penetration, Q_{gw} is groundwater runoff (mm), and t is time (day).

For rainfall-runoff analysis, the SWAT model is structured into several sub-basins, each of which is further subdivided into Hydrologic Response Units (HRUs) based on different soil types, land use and topography. Each HRU independently simulates parts of the hydrological



193 cycle, allowing a granular analysis of basin hydrology. This setup reflects the spatial
194 heterogeneity within the basin and allows continuous simulation of hydrological processes over
195 long time periods, enhancing the utility of the model for climate change studies. The model
196 was calibrated and validated using R-SWAT for parameter optimization. R-SWAT
197 incorporates the SUFI-2 algorithm, which is known for its rapid execution and precision in
198 parameter optimization, ensuring accurate and reliable simulation results (Nguyen et al., 2022).

199

200 **2.4 Streamflow drought index (SDI)**

201 The drought index was used to classify hydrological conditions considering the calibration
202 effect of periods with different hydrological conditions. SDI is a commonly used method for
203 quantifying the severity and duration of drought conditions in a river basin. It is based on the
204 comparison of observed streamflow with a historical reference period, usually the average
205 streamflow over a long-term period. SDI which is a hydrological drought index, is calculated
206 as Eq. 2. (Nalbantis and Tsakiris, 2009).

207

$$208 \quad SDI_{i,k} = \frac{V_{i,k} - \bar{V}_k}{S_k} \quad (2)$$

209

210 where $V_{i,k}$ is the runoff accumulated during the k th period in the i th year, and \bar{V}_k and S_k
211 represent the average and standard deviation of the accumulated river flow, respectively.

212 The critical level is mainly the average \bar{V}_k . In small scale rivers, the runoff rate approximates
213 the Log-normal distribution type and the probability distribution type is distorted. Therefore,
214 the runoff rate must be converted to fit the normal distribution. When converting to a two-
215 variable log-normal distribution type, SDI is finally equal to Eq. 3, and $y_{i,k}$ is a value obtained
216 by taking the natural logarithm of the amount of river water, such as Eq. 4.

217

$$218 \quad SDI_{i,k} = \frac{y_{i,k} - \bar{y}_k}{s_{y,k}}, i = 1, 2, \dots, k = 1, 2, 3, 4 \quad (3)$$

219

$$220 \quad y_{i,k} = \ln(V_{i,k}), I = 1, 2, \dots, K = 1, 2, 3, 4 \quad (4)$$



221

222 To classify the hydrological conditions, this study categorized -0.5 and below as Dry, 0.5 and
223 above as Wet, and -0.5 to 0.5 as Normal (Nalbantis and Tsakiris, 2009; Hong et al., 2015).

224

225 **2.5 General Circulation Models (GCMs)**

226 In this study, M1 to M20 GCMs from the CMIP6 suite that have been consistently used in
227 studies for East Asia and Korea were selected for future runoff projection and hydrological
228 drought analysis. The details of the development institutions, model names and resolutions of
229 these 20 GCMs were presented in Table S2.

230 The climate data from the GCMs were evaluated using daily observed climate data provided
231 by the Korea Meteorological Administration (KMA). The evaluation used observed data from
232 the past period (1985-2014) to evaluate the future climate data from the GCMs, which were
233 analyzed for two future periods: the near future (NF) and the distance future (DF). The future
234 climate change scenarios used were SSP2-4.5, SSP3-7.0 and SSP5-8.5. The SSP scenarios are
235 divided into five pathways based on radiative forcing, reflecting different levels of future
236 mitigation and adaptation efforts (O'Neill et al., 2016). The SSPs are numbered from SSP1 to
237 SSP5, with SSP1 representing a sustainable green pathway and SSP5 representing fossil fuel
238 driven development. The numbers 4.5 to 8.5 indicate the level of radiative forcing (4.5: 4.5 W
239 m⁻², 7.0: 7.0 W m⁻² and 8.5: 8.5 W m⁻²).

240

241 **2.6 Bias correction using quantile mapping**

242 The GCMs data outputs in a gridded format with a fixed resolution, requiring the use of spatial
243 interpolation methods. In this study, the inverse distance weighting (IDW) method was
244 employed to spatially interpolate the GCM data based on the locations of the Korea
245 Meteorological stations. Subsequently, to align the GCM data with the actual observational
246 data, the quantile mapping method was utilized. This method adjusts the GCM data based on
247 the quantile relationship between the cumulative distribution functions (cdf) of the GCM data
248 and the observed data (Gudmundsson et al., 2012). The quantile mapping method is described
249 by Eq (5).

250



251 $P_o = F_o^{-1}(F_m(P_m))$ (5)

252

253 where, P_o and P_m represent observed and simulated climate variables, F_m is the CDF of P_m
254 and F_o^{-1} is the inverse CDF corresponding to P_o .

255 The quantile relationship can be also derived directly using parametric transformations. In this
256 study, the linear method of parametric transformation was adopted as Eq. (6).

257

258 $\hat{P} = a + bP_m$ (6)

259

260 where, \hat{P} represents the best estimate of P_o and a and b are free parameters that are subject
261 to calibration.

262

263 **2.7 Quantifying uncertainty**

264 The ANOVA used in this study is an effective statistical method that decomposes the total sum
265 of squares (SST) into contributions from different sources and their interactions. This method
266 would be particularly useful in the study framework, as it allows us to assess not only the
267 individual effects of each source of uncertainty but also the combined effects of these sources
268 interacting with each other (Bosshard et al., 2013; Lee et al., 2021a).

269 For this analysis, the primary sources of uncertainty considered are General Circulation Models
270 (GCMs), Shared Socioeconomic Pathway (SSP) scenarios, hydrological conditions (HC)
271 during the calibration period, and period length (PL). Each of these sources could have a
272 significant impact on the projections of hydrological models; therefore, their comprehensive
273 evaluation is crucial (Morim et al., 2019; Yip et al., 2011). Higher-order interactions (e.g.,
274 three-way) were excluded as they are often difficult to interpret physically and can introduce
275 noise into the model.

276

277 $SST = SS_{GCMs} + SS_{SSPs} + SS_{HC} + SS_{PL} + SS_{Interactions(2-way)} + SS_{Residuals}$ (7)

278



279 where each term (SS) indicates the sum of squares attributed to each factor or interaction.
280 Here, SS_{GCMs} , SS_{SSPs} , SS_{HC} , and SS_{PL} represent the sum of squares due to GCMs, SSPs, HC,
281 and PL, respectively, known as the main effects. The remaining terms represent the sum of
282 squares due to the interactions among GCMs, SSPs, hydrological conditions, period length,
283 their two-way interactions, and the residual error.

284 The model setup for ANOVA considered 20 GCMs, three SSP scenarios, three hydrological
285 conditions, and different calibration period lengths. This resulted in a total of 120 unique
286 combinations for each basin analyzed. Initially, the SST, representing the total variation within
287 the data, was calculated. Subsequently, the sum of squares attributable to each source of
288 uncertainty was computed. To quantify the relative impact of each source, its contribution was
289 calculated as the proportion of its Sum of Squares relative to the Total Sum of Squares. This
290 provides a clear measure of the percentage of total uncertainty explained by each factor and
291 interaction.

292 The statistical robustness and validity of the ANOVA models were rigorously evaluated. First,
293 the overall goodness-of-fit for each model was assessed using the Adjusted R-squared (R_{adj}^2),
294 defined as Eq. (8).

295

$$296 \quad R_{adj}^2 = 1 - \frac{(1-R^2)(n-1)}{n-k-1} \quad (8)$$

297

298 Where, R^2 is the coefficient of determination, n is the number of observations, and k is the
299 number of predictors. This metric is preferred over the Standard R-squared as it adjusts for
300 the number of predictors in the model, providing a more accurate measure of model fit.

301 Second, a residual analysis was conducted to verify that the core assumptions of ANOVA were
302 met. The normality of residuals was a primary focus of this validation, examined both
303 statistically with the Shapiro-Wilk test and visually using Quantile-Quantile (Q-Q) plots. The
304 Shapiro-Wilk test evaluates the null hypothesis that the residuals are normally distributed.
305 However, given the large sample size in this study, which can lead to statistically significant
306 results even for minor deviations from normality, greater emphasis was placed on the visual
307 inspection of Q-Q plots to assess practical adherence to the normality assumption. The
308 assumption of homoscedasticity (constant variance of residuals) was also inspected using



309 Residuals vs. Fitted values plots. These validation steps ensure that the results of the
310 uncertainty partitioning are statistically sound and reliable. All statistical analyses were
311 performed using the R software environment.

312

313 **3. Results**

314 **3.1 Determining the hydrological conditions**

315 The calculated SDI was shown in Fig. S. 1. The SDI values of AD and HC in the Nakdong
316 River basin showed drought conditions similar to the actual events that occurred in 1994-1995,
317 2009, 2014-2015, 2016, 2017 and 2022 (Karunakalage et al., 2024). Similarly, SDI values of
318 CJ in the Han River basin accurately reflected the actual drought events of 2014-2015 and 2017
319 (Lee et al., 2021b). Finally, those of SJ in the Seomjin River basin also represented the drought
320 events of 1995, 2005-2006 and 2018-2019, demonstrating that the SDI was accurately
321 calculated. Therefore, this study using the observed inflow data of the four basins could reflect
322 the hydrological drought characteristics of the historical periods in South Korea.

323

324 **3.2 SWAT parameter calibration**

325 The simulated runoff data were analyzed for performance using the Kling-Gupta Efficiency
326 (KGE; Gupta et al., 2009). KGE was developed to overcome some limitations of the commonly
327 used Nash-Sutcliffe Efficiency (NSE) in performance analysis (Gupta et al., 2009). The
328 attributes of KGE include focusing on a few basic required properties of any model simulation:
329 (i) bias in the mean, (ii) bias in the variability, and (iii) cross-correlation with the observational
330 data (measuring differences in hydrograph shape and timing). The parameter optimization of
331 SWAT was performed as shown in Fig. S. 2, considering the data length of the calibration
332 period from 1 to 20 years.

333 Following parameter optimization, KGE values as shown in Fig. 2 were found to be suitable
334 for conducting the study, with all four dam basins achieving values above 0.60. The
335 performance improvements are as follows: AD's KGE increased from 0.55 before calibration
336 to 0.64 after calibration, CJ's from 0.68 to 0.75, HC's from 0.70 to 0.80, and SJ's from 0.50 to
337 0.73. This improvement in KGE after calibration underscores the robustness of the
338 hydrological models used and their enhanced capability in projecting future runoff.

339



340 **3.3 Effect of varying data length**

341 The validation performance according to the calibration data length was shown in Fig. 3. The
342 impact of calibration data length on validation performance was analyzed, revealing a departure
343 from previous studies, which suggested that longer calibration data lengths lead to more
344 effective optimization of hydrological model parameters. Instead, the influence of calibration
345 data length on performance is all different by basin. For AD, the best performance was
346 observed with a 2-year period, averaging a KGE of 0.66, while the 1-year period resulted in
347 the lowest performance with an average KGE of 0.48. The Inter Quartile Range (IQR) showed
348 that variations were smaller for periods longer than 10 years (average IQR of 0.15) compared
349 to those less than 10 years (average IQR of 0.20). For CJ, the optimal performance was at a 15-
350 year period with an average KGE of 0.72, and the lowest at a 4-year period with an average
351 KGE of 0.58. The IQR values were 0.19 for periods under 10 years and 0.20 for periods over
352 10 years, indicating minor differences due to length. For HC, the highest KGE of 0.77 was
353 recorded at 19 years, and the lowest KGE of 0.66 at 1 year. The IQR for periods under 10 years
354 was 0.19, and 0.10 for those over 10 years, showing that longer periods yielded less variability.
355 In the case of SJ, a 9-year period had a KGE of 0.68, and a 20-year period had a KGE of 0.60,
356 with IQRs of 0.23 for periods under 10 years and 0.21 for those over. While the best validation
357 performance due to calibration data length varied by basin, it was observed that the differences
358 due to the period decrease as the length increases.

359

360 **3.4 Effect of varying hydrological conditions**

361 The performance analyses based on the hydrological conditions of the calibration and
362 validation periods are shown in Fig. S. 3 and Table 1. Fig. S. 3 shows the KGE values and the
363 confidence level (prediction) for each hydrological condition during the validation period
364 according to the SDI values. Overall, during the dry and normal validation periods, it was
365 analyzed that lower SDI values (dry condition) correlated with higher KGE values. This
366 indicates that SWAT parameters calibrated with dry validation period data effectively simulate
367 runoff under Dry and Normal hydrological conditions. For wet validation periods, higher SDI
368 values (wet condition) correlate with higher KGE values, indicating that SWAT parameters
369 calibrated with wet calibration period data accurately simulate runoff under wet conditions.

370 As shown in Table 1, the average KGE according to hydrological conditions is as follows. The
371 KGE values for each dam basin, according to the hydrological conditions of the calibration-



validation periods, are as follows: For AD, D-D (Dry-Dry; hydrological conditions for calibration and validation periods, respectively) was 0.480, higher than W-D (Wet-Dry) of 0.382; D-N (Dry-Normal) was 0.573, higher than W-N (Wet-Normal) of 0.510; and W-W (Wet-Wet) was 0.642, higher than D-W (Dry-Wet) of 0.571. For CJ, D-D was 0.743, higher than W-D at 0.725; D-N was 0.643, higher than W-N at 0.615; and W-W was 0.706, higher than D-W at 0.674. For HC, D-D was 0.732, higher than W-D at 0.670; D-N was 0.738, higher than W-N at 0.714; and W-W was 0.769, higher than N-W (Normal-Wet) at 0.757. Lastly, for SJ, D-D was 0.557, higher than W-D at 0.515; D-N was 0.677, higher than W-N at 0.650; and W-W was 0.684, higher than D-W at 0.674.

The performance evaluation classified by data length and hydrological conditions for validation are influenced by hydrological conditions for calibration, but the optimal data length for the best performance varies between basins as shown in Fig. 4. These results confirm the importance of uncertainty in hydrological models due to differences in hydrological conditions during the calibration and validation periods, as suggested by previous studies (Bai et al., 2022; Fowler et al., 2016). Furthermore, the different data lengths with high validation performance for each basin confirm the opinion that shorter calibration data lengths can be applied under limited data conditions (Perrin et al., 2007; Yu et al., 2023), instead of the traditional opinion that longer calibration data lengths are better for hydrological modelling (Arsenault et al., 2018; Kim et al., 2011).

3.5 Bias correction for GCMs

In this study, climate data from GCMs were bias-corrected using observed climate data from KMA weather stations located within each dam basin. Fig. S. 4 describes the root mean square error (RMSE), Pearson coefficient and standard deviation (SD) in a Taylor diagram. After bias correction, all GCMs' climate data showed improved performance. The Pearson coefficient of precipitation increased from 0.04 to 0.99 and the RMSE decreased from 4.43 to 0.05. Similarly, the Pearson coefficients of the daily maximum and minimum temperatures averaged 1.00 and their RMSEs averaged 0.08. This is an indication that the GCM's climate data after bias correction were appropriate for use in this study.

3.6 Projection of climate variable



403 The future climate data from bias-corrected GCMs were depicted in Fig. 5 and Table S3. The
404 future period was divided into NF and FF, and it was found that daily precipitation, maximum
405 temperature, and minimum temperature all increased overall. Except for July and August,
406 future precipitation generally increased, with significant rises particularly noted in April and
407 May. In NF, the largest increase occurred in May under SSP2-4.5 with 51.4 mm, while in DF,
408 the largest increase occurred in April under SSP5-8.5 with 59.8 mm. The largest decrease in
409 NF was calculated for July under SSP5-8.5, and in DF it was most significant under SSP3-7.0,
410 indicating considerable uncertainties in the GCMs during July and August, the months of the
411 highest precipitation.

412 With regard to maximum temperatures, the analysis shows that there has been an increase in
413 all months except April in NF, especially in fall (September-November). This increase was
414 more pronounced in the DF than in the NF, with the largest increases observed under SSP5-
415 8.5. Similarly, the minimum temperature was found to have increased in the future compared
416 to the past, following the same trend as the maximum temperature.

417

418 **3.7 Projection future runoff**

419 **3.7.1 Annual runoff change**

420 The future runoff was projected using climate data and hydrological model parameters as
421 shown in Fig. S. 5. Overall, future runoff is expected to increase relative to the historical data,
422 with more significant increases projected during DF than NF. As the SSPs change (e.g. from
423 SSP2-4.5 and SSP3-7.0 to SSP5-8.5), not all annual runoff show a consistent increase with the
424 scenario change, as shown in Table 2. In particular, the increase in annual runoff under SSP5-
425 8.5 was not always higher than SSP2-4.5 or SSP3-7.0. These differences were analyzed to vary
426 significantly between different basins and GCMs.

427 For AD, the future seasonal runoff is likely to increase in all seasons except summer. This
428 increase would be more pronounced during DF than NF, with the largest increases occurring
429 under SSP5-8.5. For CJ, the future runoff is expected to increase compared to the past in all
430 seasons, with the highest increase observed in DF under SSP3-7.0 and the lowest increase
431 under SSP5-8.5. For HC, future runoff is expected to increase in all seasons except fall, with
432 the greatest variability in fall under SSP3-7.0. For SJ, future runoff is projected to increase
433 compared to the past in all scenarios except NF under SSP3-7.0.



434

435 3.7.2 Differences in projected future runoff due to hydrological model parameters

436 The future runoff projections using many calibrated sets of hydrological model parameters
437 were analyzed using the flow duration curve (FDC). In water resources planning and drought
438 management, the differences in future runoff projections due to hydrological model parameters
439 at low runoff are critical. These differences are shown in Fig. S. 6, and the differences in Q75
440 for each basin and their proportions relative to the mean runoff are shown in Table 3. The basin
441 with the largest differences due to hydrological conditions in the calibration period was
442 analysed as HC. HC is a basin with relatively low precipitation and a small watershed area. CJ,
443 the largest basin, was analysed to have a 5-6% difference in runoff by hydrological model
444 parameters, which means that the effect of hydrological model calibration is larger in smaller
445 basins. The overall trend shows larger variances in DF than NF, and these variances were more
446 pronounced for SSP5-8.5 scenario than SSP2-4.5. This indicates the need to consider the
447 variations caused by hydrological model parameters when managing water resources during
448 both flood and drought periods. Table S4 details the top three GCMs that showed the most
449 significant differences in runoff projections due to hydrological model parameters for each
450 basin. Models, M5 and M6 were consistently identified as having the largest discrepancies in
451 future runoff projections due to hydrological model parameters.

452

453 **3.8 Uncertainty contribution of future runoff projections**

454 3.8.1 Statistical significance of ANOVA results for future runoff projection

455 Before assessing the significance of individual uncertainty sources, the statistical validity of
456 the developed ANOVA models was confirmed. The goodness-of-fit for all monthly models
457 across all four basins and both future periods (NF and DF) were exceptionally high, with
458 Adjusted R-squared values consistently exceeding 0.99. This indicates that the selected factors
459 and their two-way interactions explain more than 99% of the variance in the projected future
460 runoff. Furthermore, a comprehensive residual analysis was conducted for each model. While
461 statistical tests for normality, such as the Shapiro-Wilk test, are sensitive to large sample sizes,
462 the visual inspection of Q-Q plots and Residuals vs. Fitted plots confirmed that the assumptions
463 of normality and homoscedasticity were practically satisfied, ensuring the reliability of the
464 subsequent significance testing (Fig. S. 7-8).



465 The factors related to the hydrological model calibration, HC and PL, were also found to be
466 statistically significant for the future runoff projections. Table 4-5 summarizes the frequency
467 of statistical significance ($p < 0.05$) for each factor across the four study basins. The values
468 indicate the number of basins out of four where the factor was found to be significant. Although
469 their influence was smaller than that of GCMs and SSPs, both HC and PL were significant (p
470 < 0.05) in numerous months, particularly during the low-flow periods such as spring and winter.
471 This result highlights that the calibration conditions should be considered an important source
472 of uncertainty.

473 Among the two-way interactions, the GCM:SSP interaction consistently showed the highest
474 statistical significance ($p < 0.001$) across all months and basins, indicating that the effect of a
475 GCM is strongly dependent on the chosen SSP scenario, and vice versa. Furthermore,
476 interactions involving the calibration factors, such as GCM:HC and HC:PL, were also found
477 to be statistically significant in various months. This finding is crucial as it demonstrates that
478 the uncertainty stemming from hydrological model calibration does not act in isolation but
479 interacts in a complex manner with future climate projections, thereby influencing the overall
480 uncertainty of future runoff.

481

482 3.8.2 Contribution of uncertainty using the ANOVA

483 Fig. S. 9 shows the relative contributions of different factors to the uncertainties in future runoff
484 projections for each basin. Fig. 6 specifically highlights the uncertainty contributions attributed
485 to hydrological models. The differences in future climate data from the GCMs were found to
486 be the largest source of uncertainty, contributing over 60%. This is more significant during NF
487 than DF, due to the increased climate variability in GCM projections during the NF, as
488 discussed in Section 3.6.

489 The uncertainty contributions from hydrological models were most significant during the
490 spring (Mar-May) and winter (Dec-Feb) periods, as shown in Table S5. The results of the
491 analysis for each basin were as follows: For AD, the hydrological model uncertainty was most
492 significant in spring (NF: 7.54%, and DF: 5.86%), with a maximum of 9.76% in June for NF
493 and 7.54% in April for DF. In CJ, the highest uncertainties were also found for NF in winter
494 (3.9%) and for DF in spring (3.96%). HC showed the highest uncertainty in winter (NF: 6.09%,
495 and DF: 5.5%), with a maximum in November (NF: 9.76%, and DF: 8.92%). For SJ, the most



496 significant contributions were found in spring (NF: 5.58%, and DF: 3.88%). In the end,
497 hydrological model uncertainties were more significant in months with lower runoff.

498

499 **3.9 Future hydrological drought uncertainty**

500 **3.9.1 Future hydrological drought uncertainty according to hydrological conditions**

501 To quantify the uncertainty in the future hydrological drought analysis using the calibrated sets
502 of hydrological model parameters, the Streamflow Drought Index (SDI) was used to calculate
503 the hydrological drought conditions during the future period. For the uncertainty analysis,
504 runoff data were considered for both historical and future periods. Table 6 shows the difference
505 in the number of drought events under hydrological conditions during the calibration period
506 after calculating SDIs for 3-month, 6-month, and 12-month durations. The difference in the
507 number of drought events according to the hydrological conditions of the calibration period
508 was analysed differently for each SSP and basin. The difference was significant for the shorter
509 duration of 3 months.

510 According to the analysis by basin, the difference in the number of drought events in the AD
511 basin with a 3-month duration was calculated to be the largest, with an average of 4.93 events,
512 followed by SJ, CJ, and HC. Between the near future (NF) and distant future (DF), the
513 difference in the number of drought events under the overall hydrological conditions was larger
514 in the NF, and this difference was calculated differently by basin, confirming the need for
515 basin-specific analysis in water resource management planning. Therefore, the uncertainty
516 quantification of the drought analysis was performed using the SDI with a duration of 3 months.

517

518 **3.9.2 Statistical significance of ANOVA results for future hydrological drought**

519 To confirm the statistical validity of the ANOVA models for the future hydrological drought
520 analysis, the goodness-of-fit was evaluated. The models showed a high goodness-of-fit, with
521 Adjusted R-squared values consistently greater than 0.99 for all annual models across the four
522 basins. This indicates that the selected factors and their two-way interactions explain more than
523 99% of the variance in the future drought projections, ensuring the reliability of the analysis.

524 Table 7 summarizes the frequency of statistical significance ($p < 0.05$) for each factor,
525 aggregated by decade, to provide a concise overview of the results across the entire future



526 period. The values indicate the number of basins (out of four) where the factor was found to be
527 significant for the majority of years within that decade. The primary climate-related factors,
528 GCM and SSP, were consistently identified as the most significant sources of uncertainty. As
529 shown in Table 7, both factors were found to be highly significant across all four basins for all
530 decades, underscoring the profound impact of climate model choice and emission scenarios on
531 drought projections.

532 The hydrological model calibration factors, HC and PL, also proved to be important sources of
533 uncertainty. Both factors were statistically significant across all four basins for the entire future
534 period. This finding reinforces that the hydrological conditions and data length used for model
535 calibration have a persistent and significant influence on long-term hydrological drought
536 assessments.

537 Regarding the interaction effects, the GCM:SSP interaction was the most consistently
538 significant, highlighting that the projected drought severity under a specific GCM is highly
539 dependent on the emission scenario. Moreover, interactions involving calibration factors,
540 particularly GCM:HC, GCM:PL, and HC:PL, were also found to be statistically significant
541 across all basins and decades. This indicates that the uncertainty from calibration conditions
542 does not merely add to the total uncertainty but also modulates the uncertainty stemming from
543 climate models, which is a critical consideration for developing robust drought management
544 strategies. In contrast, other interactions such as SSP:HC and SSP:PL were found to be not
545 significant across the basins and decades.

546

547 3.9.3 Uncertainty contribution of future hydrological drought

548 The quantification of uncertainty in future hydrological drought was conducted using
549 ANOVA. The uncertainty in future hydrological drought projections caused by SSP, GCM,
550 and hydrological modelling parameters was clearly quantified by ANOVA. Fig S.10 shows
551 the contribution of each factor to the total uncertainty. Among single-factor uncertainties,
552 GCM contributed the most, averaging over 30%. The largest contributor to the total
553 uncertainty, however, was the interaction between SSP and GCM, averaging over 50%.

554 Fig. 7 and Table 8 present the contribution of hydrological modelling parameters to the
555 uncertainty in future drought projections. The uncertainty contribution from hydrological
556 model parameter estimation in future hydrological drought analysis averaged 2.7%, which is



557 lower than that observed for future runoff projections. The uncertainty contribution from
558 hydrological model calibration for future drought conditions was highest in HC, followed by
559 CJ, AD, and SJ, respectively. These results differ from those obtained in the runoff
560 projections. The contribution of uncertainty in hydrological drought analysis decreased for
561 AD and SJ, where uncertainty in future runoff projection due to hydrological model
562 calibration was relatively high. In contrast, HC showed high uncertainty contributions from
563 hydrological model calibration in both runoff and drought analyses. For CJ, uncertainty from
564 hydrological model calibration was relatively low in future runoff projections but increased in
565 the hydrological drought analysis. These findings confirm the necessity to separately analyze
566 and consider uncertainties in future runoff projection and hydrological drought analysis.

567

568 **4. Discussion**

569 This study quantified the cascade of uncertainties caused by various factors in the process of
570 projecting future runoff and analyzing future hydrological drought. Previous studies
571 (Chegwidden et al., 2019; Wang et al., 2020) have reported that climate data from GCMs and
572 SSP scenarios are the primary sources of uncertainty in future hydrological analysis. The
573 results of this study also identified GCMs as the major contributor to uncertainty in future
574 hydrological analysis. However, recent research has begun to identify and quantify the
575 cascade of uncertainties caused by factors beyond GCMs and SSP scenarios (Chen et al.,
576 2022; Shi et al., 2022). This study focused on the uncertainties inherent in the calibration of
577 hydrological models, which are essential for future water resource management.

578 There have been limited studies that consider the uncertainties in runoff projection due to
579 various calibrated parameter cases (Lee et al., 2021a). However, this study further subdivided
580 the observation data used in the calibration period of hydrological model parameters by the
581 amount of data and hydrological conditions to quantify the uncertainties more precisely. The
582 results showed that hydrological conditions had a greater impact than the amount of
583 calibration data period on the uncertainties in the calibration of hydrological model
584 parameters.

585 This study went beyond merely projecting future runoff by also quantifying the cascade of
586 uncertainties in the analysis of future hydrological drought using this runoff projection. Many
587 studies on future drought prediction reported that hydrological drought becomes more
588 complex and uncertain due to its association with human activities and the use of future



589 climate data and hydrological models (Ashrafi et al., 2020; Satoh et al., 2022). Most existing
590 studies on future hydrological drought analysis focused on the severity and frequency of
591 droughts. However, this study quantified the cascade of uncertainties that arise in the process
592 of future drought analysis. Although the contribution of hydrological model uncertainty to
593 future hydrological drought may be lower compared to future runoff projections, the
594 characteristics of uncertainty differ between drought and runoff projections, clearly indicating
595 the necessity to separately analyze and consider these uncertainties in future hydrological
596 analyses.

597

598 **5. Conclusion**

599 This study aimed to quantify the uncertainties in future runoff projections and hydrological
600 drought analysis, considering various climate change scenarios and hydrological model
601 calibrations. The SWAT model was used, and hydrological conditions were classified using
602 the SDI. Additionally, 20 GCMs and three SSP scenarios were applied. The calibration data
603 length ranged from 1 to 20 years, considering different hydrological conditions (Dry, Normal,
604 Wet).

605 The main findings are as follows:

606 First, the validation performance of the calibrated hydrological model parameters depended
607 significantly on the hydrological conditions of the calibration data. The hydrological model
608 parameters calibrated with dry period data showed 11.4% higher performance under dry
609 conditions and 6.1% higher performance under normal conditions.

610 Second, the contribution of hydrological model uncertainty to future runoff projections
611 ranged from 3.9% to 9.8%, with this uncertainty being more pronounced during low runoff
612 periods. ANOVA results clearly indicated that GCMs contributed the most uncertainty,
613 consistently accounting for over 60% on average, highlighting GCMs as the dominant source.
614 In contrast, the contributions of SSP scenarios and hydrological model parameters were
615 relatively smaller.

616 Third, the contribution of hydrological model uncertainty in future hydrological drought
617 analysis was on average 2.7%, lower than that observed for future runoff projections. The
618 uncertainty contributions varied by basin, showing different patterns from runoff projections,



619 thus confirming the necessity for separate analyses of future runoff and hydrological drought
620 uncertainties.

621 The significance of this study lies in emphasizing the quantification of uncertainty from
622 various sources, including hydrological conditions and calibration data length, in addition to
623 climate model scenarios. The systematic approach using ANOVA provided insights into the
624 dominant sources and interactions of uncertainties, offering important guidance for
625 improving hydrological modeling practices and water resources planning under future climate
626 scenarios. However, there remains a need to apply this methodology to other regions to
627 generalize these findings further.

628

629 **Competing interests**

630 The contact author has declared that none of the authors has any competing interests.

631 **Acknowledgement**

632 This study was supported by of National Research Foundation of Korea
633 (2021R1A2C2005699).

634

635 **References**

- 636 Abdulai, P. J., Chung, E.S.: Uncertainty assessment in drought severities for the
637 Cheongmicheon watershed using multiple GCMs and the reliability ensemble averaging
638 method, *Sustainability*, 11(16), 4283, <https://doi.org/10.3390/su11164283>, 2019
- 639 Arsenault, R., Brisette, F., & Martel, J. L.: The hazards of split-sample validation in
640 hydrological model calibration, *J Hydrol*, 566, 346-362,
641 <https://doi.org/10.1016/j.jhydrol.2018.09.027>, 2018
- 642 Ashrafi, S. M., Gholami, H., & Najafi, M. R.: Uncertainties in runoff projection and
643 hydrological drought assessment over Gharezu basin under CMIP5 RCP
644 scenarios, *J Water Clim Chang*, 11(S1), 145-163, <https://doi.org/10.2166/wcc.2020.088>, 2020
- 645 Bai, P., Liu, X., & Xie, J.: Simulating runoff under changing climatic conditions: a
646 comparison of the long short-term memory network with two conceptual hydrologic
647 models, *J Hydrol*, 592, 125779, <https://doi.org/10.1016/j.jhydrol.2020.125779>, 2021



- 648 Bosshard, T., Carambia, M., Goergen, K., Kotlarski, S., Krahe, P., Zappa, M., & Schär, C.:
649 Quantifying uncertainty sources in an ensemble of hydrological climate-impact
650 projections, *Water Resour Res*, 49(3), 1523-1536, <https://doi.org/10.1029/2011WR011533>,
651 2013
- 652 Broderick, C., Matthews, T., Wilby, R. L., Bastola, S., & Murphy, C.: Transferability of
653 hydrological models and ensemble averaging methods between contrasting climatic
654 periods, *Water Resour Res*, 52(10), 8343-8373, <https://doi.org/10.1002/2016WR018850>,
655 2016
- 656 Chae, S. T., Chung, E. S., & Jiang, J.: Enhancing Water Cycle Restoration through LID
657 Practices Considering Climate Change: A Study on Permeable Pavement Planning by an
658 Iterative MCDM Model, *Water Resour Manag*, 38(9), 3413-3428,
659 <https://doi.org/10.1007/s11269-024-03821-z>, 2024
- 660 Chae, S.T. Chung, E.S., Kim, D.: Evaluation of optimized multi-model ensembles for
661 extreme precipitation projection considering various objective functions, *Water Resour*, 1-19,
662 <https://doi.org/10.1007/s11269-024-03948-z>, 2024
- 663 Chegwiddden, O. S., Nijssen, B., Rupp, D. E., Arnold, J. R., Clark, M. P., Hamman, J. J., Kao,
664 S.-C., Mao, Y., Mizukami, N., Mote, P.W., Pan, M., Pytlak, E., & Xiao, M.: How do
665 modeling decisions affect the spread among hydrologic climate change projections?
666 Exploring a large ensemble of simulations across a diversity of hydroclimates, *Earths*
667 *Future*, 7(6), 623-637, <https://doi.org/10.1029/2018EF001047>, 2019
- 668 Chen, C., Gan, R., Feng, D., Yang, F., & Zuo, Q.: Quantifying the contribution of SWAT
669 modeling and CMIP6 inputting to streamflow prediction uncertainty under climate change, *J*
670 *Clean Prod*, 364, 132675, <https://doi.org/10.1016/j.jclepro.2022.132675>, 2022
- 671 Coron, L., Andréassian, V., Perrin, C., Lerat, J., Vaze, J., Bourqui, M., & Hendrickx, F.:
672 Crash testing hydrological models in contrasted climate conditions: An experiment on 216
673 Australian catchments, *Water Resour Res*, 48(5), <https://doi.org/10.1029/2011WR011721>,
674 2012
- 675 Dakhlaoui, H., Ruelland, D., Trambly, Y., & Bargaoui, Z.: Evaluating the robustness of
676 conceptual rainfall-runoff models under climate variability in northern Tunisia, *J*
677 *Hydrol*, 550, 201-217, <https://doi.org/10.1016/j.jhydrol.2017.04.032>, 2017



- 678 Devia, G. K., Ganasri, B. P., & Dwarakish, G. S.: A review on hydrological
679 models, *Aquat Procedia*. 4, 1001-1007, <https://doi.org/10.1016/j.aqpro.2015.02.126>, 2015
- 680 Feng, K., Zhou, J., Liu, Y., Lu, C., & He, Z.: Hydrological uncertainty processor (HUP) with
681 estimation of the marginal distribution by a Gaussian mixture model, *Water Resour*
682 *Manag*, 33, 2975-2990, <https://doi.org/10.1007/s11269-019-02260-5>, 2019
- 683 Fowler, K. J., Peel, M. C., Western, A. W., Zhang, L., & Peterson, T. J.: Simulating runoff
684 under changing climatic conditions: Revisiting an apparent deficiency of conceptual rainfall-
685 runoff models, *Water Resour Res*. 52(3), 1820-1846,
686 <https://doi.org/10.1002/2015WR018068>, 2016
- 687 Ghasemizade, M., & Schirmer, M.: Subsurface flow contribution in the hydrological cycle:
688 lessons learned and challenges ahead—a review, *Environ Earth Sci*. 69, 707-718,
689 <https://doi.org/10.1007/s12665-013-2329-8>, 2013
- 690 Gudmundsson, L., Bremnes, J. B., Haugen, J. E., & Engen-Skaugen, T.: Downscaling RCM
691 precipitation to the station scale using statistical transformations—a comparison of
692 methods, *Hydrol Earth Syst Sci*, 16(9), 3383-3390, [https://doi.org/10.5194/hess-16-3383-](https://doi.org/10.5194/hess-16-3383-2012)
693 2012, 2012
- 694 Gupta, H. V., Kling, H., Yilmaz, K. K., & Martinez, G. F.: Decomposition of the mean
695 squared error and NSE performance criteria: Implications for improving hydrological
696 modelling, *J Hydrol*, 377(1-2), 80-91, <https://doi.org/10.1016/j.jhydrol.2009.08.003>, 2009
- 697 Hanel, M., & Buishand, T. A.: Assessment of the sources of variation in changes of
698 precipitation characteristics over the Rhine basin using a linear mixed-effects model. *J*
699 *Clim.*, 28(17), 6903-6919, <https://doi.org/10.1175/JCLI-D-14-00775.1>, 2015
- 700 Hong, X., Guo, S., Zhou, Y., & Xiong, L.: Uncertainties in assessing hydrological drought
701 using streamflow drought index for the upper Yangtze River basin, *Stoch Environ*
702 *Res Risk Assess*, 29, 1235-1247, <https://doi.org/10.1007/s00477-014-0949-5>, 2015
- 703 IPCC: IPCC Climate Change 2014: Synthesis Report. Contribution of Working Groups I, II
704 and III to the Fifth Assessment Report of the Intergovernmental Panel on Climate Change,
705 IPCC, Geneva, Switzerland, 2014
- 706 IPCC.: Summary for Policymakers. In: *Climate Change 2021: The Physical Science Basis*.
707 Contribution of Working Group I to the Sixth Assessment Report of the Intergovernmental



- 708 Panel on Climate Change [Masson-Delmotte, V., P. Zhai, A. Pirani, S. L. Connors, C. Péan,
709 S. Berger, N. Caud, Y. Chen, L. Goldfarb, M. I. Gomis, M. Huang, K. Leitzell, E. Lonnoy,
710 J.B.R. Matthews, T. K. Maycock, T. Waterfield, O. Yelekçi, R. Yu and B. Zhou (eds.)].
711 Cambridge University Press. In Press, 2021
- 712 Karunakalage, A., Lee, J. Y., Daqiq, M. T., Cha, J., Jang, J., & Kannaujiya, S.:
713 Characterization of groundwater drought and understanding of climatic impact on
714 groundwater resources in Korea, *J Hydrol*, 634, 131014,
715 <https://doi.org/10.1016/j.jhydrol.2024.131014>, 2024
- 716 Kim, H. S., Croke, B. F., Jakeman, A. J., & Chiew, F. H.: An assessment of modelling
717 capacity to identify the impacts of climate variability on catchment hydrology, *Math Comput*
718 *Simul.* 81(7), 1419-1429, <https://doi.org/10.1016/j.matcom.2010.05.007>, 2011
- 719 Kim, J. H., Sung, J. H., Chung, E. S., Kim, S. U., Son, M., & Shiru, M. S.: Comparison of
720 Projection in Meteorological and Hydrological Droughts in the Cheongmicheon Watershed
721 for RCP4. 5 and SSP2-4.5, *Sustainability*, 13(4), 2066, <https://doi.org/10.3390/su13042066>,
722 2021
- 723 Kim, J. H., Sung, J. H., Shahid, S., & Chung, E. S.: Future hydrological drought analysis
724 considering agricultural water withdrawal under SSP scenarios, *Water Resour Manag*, 36(9),
725 2913-2930, <https://doi.org/10.1007/s11269-022-03116-1>, 2022
- 726 Lee, S., Qi, J., McCarty, G. W., Yeo, I. Y., Zhang, X., Moglen, G. E., & Du, L.: Uncertainty
727 assessment of multi-parameter, multi-GCM, and multi-RCP simulations for streamflow and
728 non-floodplain wetland (NFW) water storage, *J Hydrol*, 600, 126564,
729 <https://doi.org/10.1016/j.jhydrol.2021.126564>, 2021
- 730 Lee, S., Lee, S. J., Jang, K., & Chun, J. H.: Drought monitoring based on vegetation type and
731 reanalysis data in Korea, *Atmosphere*, 12(2), 170,
732 <https://doi.org/10.1016/j.jhydrol.2021.126564>, 2021
- 733 Mahabadi, S. A., & Delavar, M.: Evaluation and comparison of different methods for
734 determining the contribution of climatic factors and direct human interventions in reducing
735 basin discharge, *Ecol Indic*, 158, 111480, <https://doi.org/10.1016/j.ecolind.2023.111480>,
736 2024



- 737 Merz, R., Parajka, J., & Blöschl, G.: Time stability of catchment model parameters:
738 Implications for climate impact analyses, *Water Resour Res*, 47(2),
739 <https://doi.org/10.1029/2010WR009505>, 2011
- 740 Milly, P. C., Betancourt, J., Falkenmark, M., Hirsch, R. M., Kundzewicz, Z. W., Lettenmaier,
741 D. P., & Stouffer, R. J., 2008. Stationarity is dead: Whither water
742 management?. *Science*. 319(5863), 573-574.
- 743 Mo, C., Huang, K., Ruan, Y., Lai, S., & Lei, X.: Quantifying uncertainty sources in runoff
744 change attribution based on the Budyko framework, *J Hydrol*, 630, 130790,
745 <https://doi.org/10.1016/j.jhydrol.2024.130790>, 2024
- 746 Morim, J., M. Hemer, X.L. Wang, N. Cartwright, C. Trenham, A. Semedo, I. Young, L.
747 Bricheno, P. Camus, M. Casas-Prat, L.i. Erikson, L. Mentaschi, N. Mori, T. Shimura, B.
748 Timmermans, O. Aarnes, Ø. Breivik, A. Behrens, M. Dobrynin, M. Menendez, J. Staneva, M.
749 Wehner, J. Wolf, B. Kamranzad, A. Webb, J. Stopa, F. Andutta.: Robustness and
750 uncertainties in global multivariate wind-wave climate projections, *Nat Clim Chang*, 9(9),
751 711-718, <https://doi.org/10.1038/s41558-019-0542-5>, 2019
- 752 Nalbantis, I., & Tsakiris, G.: Assessment of hydrological drought revisited, *Water Resour*
753 *Manag*, 23, 881-897, <https://doi.org/10.1007/s11269-008-9305-1>, 2009
- 754 Nguyen, T. V., Dietrich, J., Dang, T. D., Tran, D. A., Van Doan, B., Sarrazin, F. J.,
755 Abbaspour, K., & Srinivasan, R.: An interactive graphical interface tool for parameter
756 calibration, sensitivity analysis, uncertainty analysis, and visualization for the Soil and Water
757 Assessment Tool, *Environ Model Softw*, 156, 105497,
758 <https://doi.org/10.1016/j.envsoft.2022.105497>, 2022
- 759 O'Neill, B. C., Tebaldi, C., Van Vuuren, D. P., Eyring, V., Friedlingstein, P., Hurtt, G.,
760 Knutti, R., Kriegler, E., Lamarque, J.F., Lowe, J., Meehl, J., Moss, R., Riahi, K., Sanderson,
761 B. M.: The scenario model intercomparison project (ScenarioMIP) for
762 CMIP6, *Geosci Model Dev*, 9(9), 3461-3482, <https://doi.org/10.5194/gmd-9-3461-2016>,
763 2016
- 764 Peng, A., Zhang, X., Xu, W., & Tian, Y.: Effects of training data on the learning performance
765 of LSTM network for runoff simulation, *Water Resour Manag t*, 36(7), 2381-2394,
766 <https://doi.org/10.1007/s11269-022-03148-7>, 2022



- 767 Perrin, C., Oudin, L., Andreassian, V., Rojas-Serna, C., Michel, C., & Mathevet, T.: Impact
768 of limited streamflow data on the efficiency and the parameters of rainfall—runoff
769 models, *Hydrol Sci J*, 52(1), 131-151, <https://doi.org/10.1623/hysj.52.1.131>, 2007
- 770 Qi, W., Zhang, C., Fu, G., Sweetapple, C., & Zhou, H.: Evaluation of global fine-resolution
771 precipitation products and their uncertainty quantification in ensemble discharge
772 simulations, *Hydrol Earth Syst Sci*, 20(2), 903-920, [https://doi.org/10.5194/hess-20-903-](https://doi.org/10.5194/hess-20-903-2016)
773 2016, 2016
- 774 Razavi, S., & Tolson, B. A.: An efficient framework for hydrologic model calibration on long
775 data periods, *Water Resour Res*, 49(12), 8418-8431, <https://doi.org/10.1002/2012WR013442>,
776 2013
- 777 Renard, B., Kavetski, D., Kuczera, G., Thyer, M., & Franks, S. W.: Understanding predictive
778 uncertainty in hydrologic modeling: The challenge of identifying input and structural
779 errors, *Water Resour Res*, 46(5), <https://doi.org/10.1029/2009WR008328>, 2010
- 780 Saft, M., Peel, M. C., Western, A. W., Perraud, J. M., & Zhang, L.: Bias in streamflow
781 projections due to climate-induced shifts in catchment response, *Geophys Res Lett*, 43(4),
782 1574-1581, <https://doi.org/10.1002/2015GL067326>, 2016
- 783 Santos, C. A. G., Neto, R. M. B., do Nascimento, T. V. M., da Silva, R. M., Mishra, M., &
784 Frade, T. G.: Geospatial drought severity analysis based on PERSIANN-CDR-estimated
785 rainfall data for Odisha state in India (1983–2018), *Sci Total Environ*, 750, 141258,
786 <https://doi.org/10.1016/j.scitotenv.2020.141258>, 2021
- 787 Satoh, Y., Yoshimura, K., Pokhrel, Y., Kim, H., Shiogama, H., Yokohata, T., Hanasaki, N.,
788 Wada, Y., Burek, P., Byers, E., Schmied, H. M., Gerten, D., Ostberg, S., Gosling, S. N.,
789 Boulange, J. E. S., & Oki, T.: The timing of unprecedented hydrological drought under
790 climate change, *Nat Commun*, 13(1), 3287, <https://doi.org/10.1038/s41467-022-30729-2>,
791 2022
- 792 Sheffield, J., & Wood, E. F.: *Drought: past problems and future scenarios*. Routledge,
793 <https://doi.org/10.4324/9781849775250>, 2012
- 794 Shi, L., Feng, P., Wang, B., Li Liu, D., Zhang, H., Liu, J., & Yu, Q.: Assessing future runoff
795 changes with different potential evapotranspiration inputs based on multi-model ensemble of



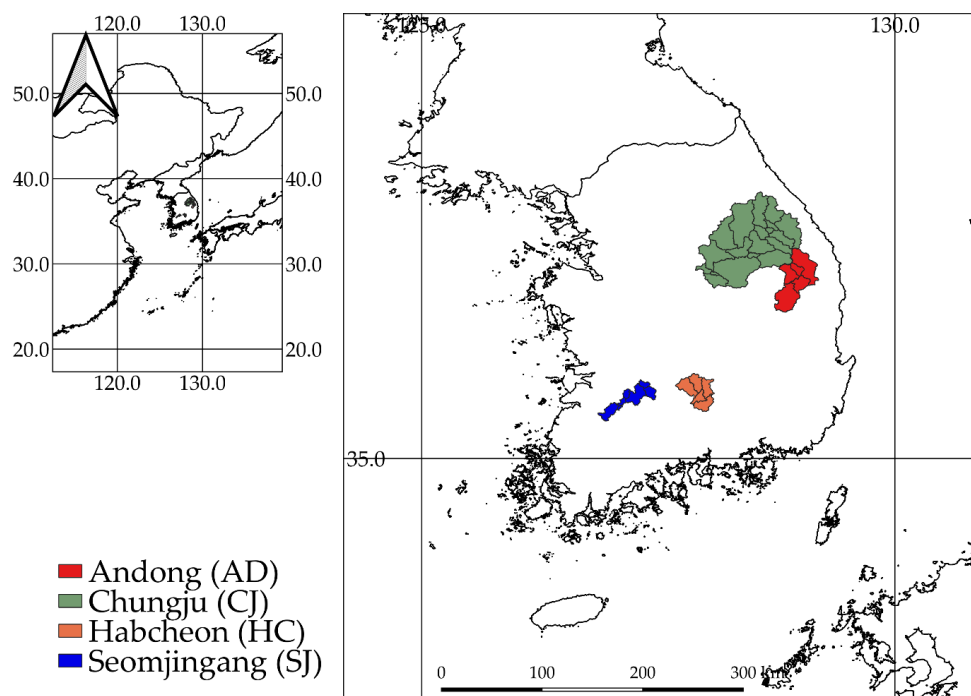
- 796 CMIP5 projections, *J Hydrol*, 612, 128042, <https://doi.org/10.1016/j.jhydrol.2022.128042>,
797 2022
- 798 Song, Y. H., Chung, E. S., & Shahid, S.: Differences in extremes and uncertainties in future
799 runoff simulations using SWAT and LSTM for SSP scenarios, *Sci Total Environ*, 838,
800 156162, <https://doi.org/10.1016/j.scitotenv.2022.156162>, 2022
- 801 Sun, W., Wang, Y., Wang, G., Cui, X., Yu, J., Zuo, D., & Xu, Z.: Physically based
802 distributed hydrological model calibration based on a short period of streamflow data: case
803 studies in four Chinese basins, *Hydrol Earth Syst Sci*, 21(1), 251-265,
804 <https://doi.org/10.5194/hess-21-251-2017>, 2017
- 805 Sung, J. H., Chung, E. S., & Shahid, S.: Reliability–Resiliency–Vulnerability approach for
806 drought analysis in South Korea using 28 GCMs, *Sustainability*, 10(9), 3043,
807 <https://doi.org/10.3390/su10093043>, 2018
- 808 Thirel, G., Andréassian, V., & Perrin, C.: On the need to test hydrological models under
809 changing conditions, *Hydrol Sci J*, 60(7-8), 1165-1173,
810 <https://doi.org/10.1080/02626667.2015.1050027>, 2015
- 811 Vetter, T., Huang, S., Aich, V., Yang, T., Wang, X., Krysanova, V., & Hattermann, F.: Multi-
812 model climate impact assessment and intercomparison for three large-scale river basins on
813 three continents, *Earth Syst Dyn*, 6(1), 17-43, <https://doi.org/10.5194/esd-6-17-2015>, 2015
- 814 Wang, H. M., Chen, J., Xu, C. Y., Zhang, J., & Chen, H.: A framework to quantify the
815 uncertainty contribution of GCMs over multiple sources in hydrological impacts of climate
816 change, *Earths Future*, 8(8), e2020EF001602, <https://doi.org/10.1029/2020EF001602>, 2020
- 817 Xu, Z., Godrej, A. N., & Grizzard, T. J.: The hydrological calibration and validation of a
818 complexly-linked watershed–reservoir model for the Occoquan watershed, Virginia, *J*
819 *Hydrol*, 345(3-4), 167-183, <https://doi.org/10.1016/j.jhydrol.2007.07.015>, 2007
- 820 Yang, G., Giuliani, M., & Galelli, S.: Valuing the codesign of streamflow forecast and
821 reservoir operation models, *J Water Resour Plan Manag*, 149(8), 04023037,
822 <https://doi.org/10.1061/JWRMD5.WRENG-6023>, 2023
- 823 Yang, X., Chen, Z., & Qin, M.: Monthly Runoff Prediction Via Mode Decomposition-
824 Recombination Technique, *Water Resour Manag*, 38(1), 269-286,
825 <https://doi.org/10.1007/s11269-023-03668-w>, 2023



- 826 Yip, S., Ferro, C. A., Stephenson, D. B., & Hawkins, E.: A simple, coherent framework for
827 partitioning uncertainty in climate predictions, *J Clim Change*, 24(17), 4634-4643,
828 <https://doi.org/10.1175/2011JCLI4085.1>, 2011
- 829 Yu, Q., Jiang, L., Wang, Y., & Liu, J., 2023. Enhancing streamflow simulation using
830 hybridized machine learning models in a semi-arid basin of the Chinese loess Plateau. *J*
831 *Hydrol.* 617, 129115.
- 832 Yuan, Q., Thorarinsdottir, T. L., Beldring, S., Wong, W. K., & Xu, C. Y.: Assessing
833 uncertainty in hydrological projections arising from local-scale internal variability of
834 climate, *J Hydrol*, 620, 129415, <https://doi.org/10.1016/j.jhydrol.2023.129115>, 2023
- 835 Zhang, X., Song, S., & Guo, T.: Nonlinear Segmental Runoff Ensemble Prediction Model
836 Using BMA, *Water Resour Manag*, 1-18, <https://doi.org/10.1007/s11269-024-03824-w>, 2024
- 837 Ziarh, G. F., Kim, J. H., Song, J. Y., & Chung, E. S.: Quantifying Uncertainty in Runoff
838 Simulation According to Multiple Evaluation Metrics and Varying Calibration Data
839 Length, *Water*, 16(4), 517, <https://doi.org/10.3390/w16040517>, 2024
- 840



841



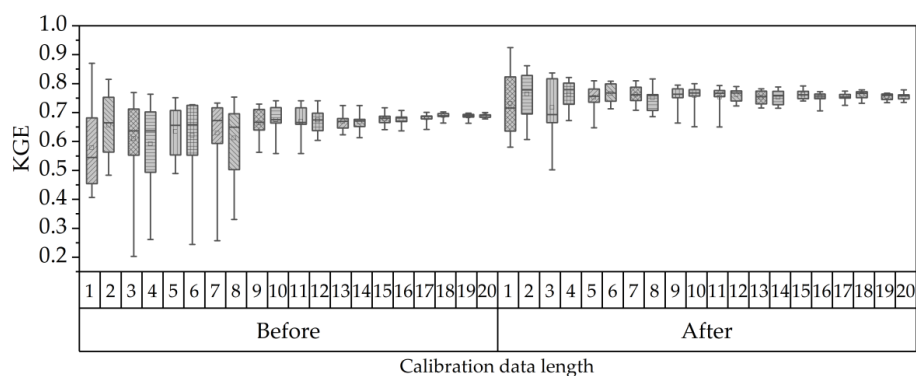
842

843 *Figure 1. Description of study area.*

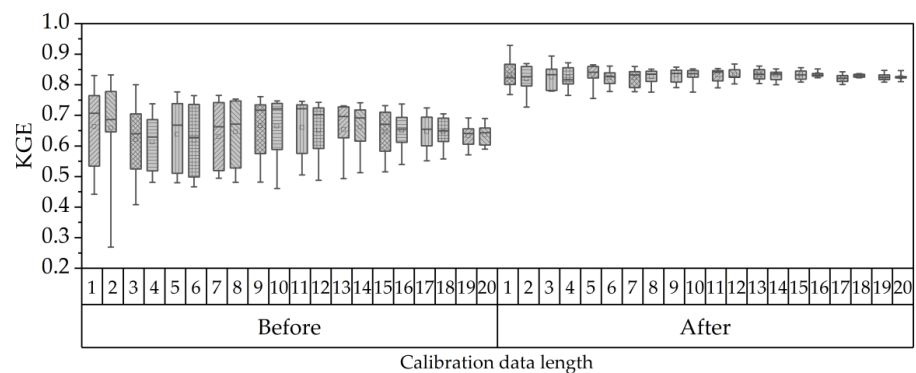
844



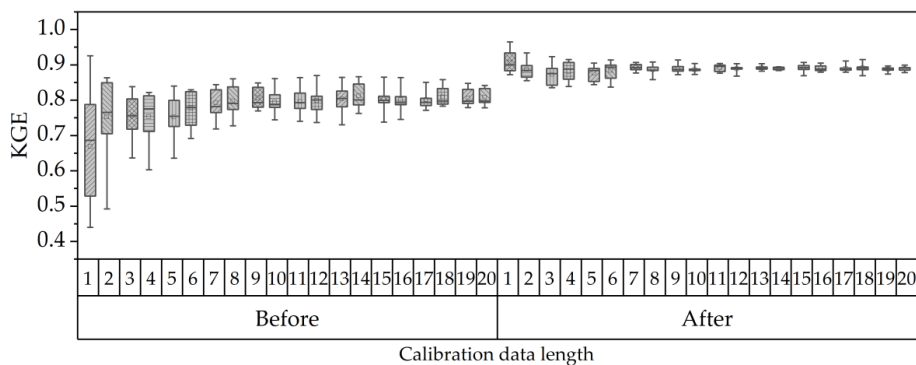
845



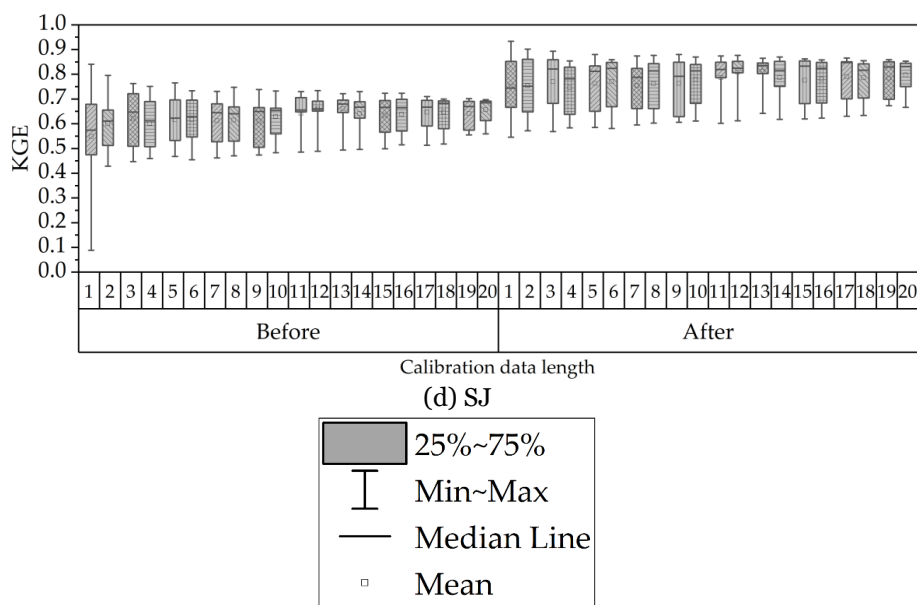
(a) AD



(b) CJ



(c) HC

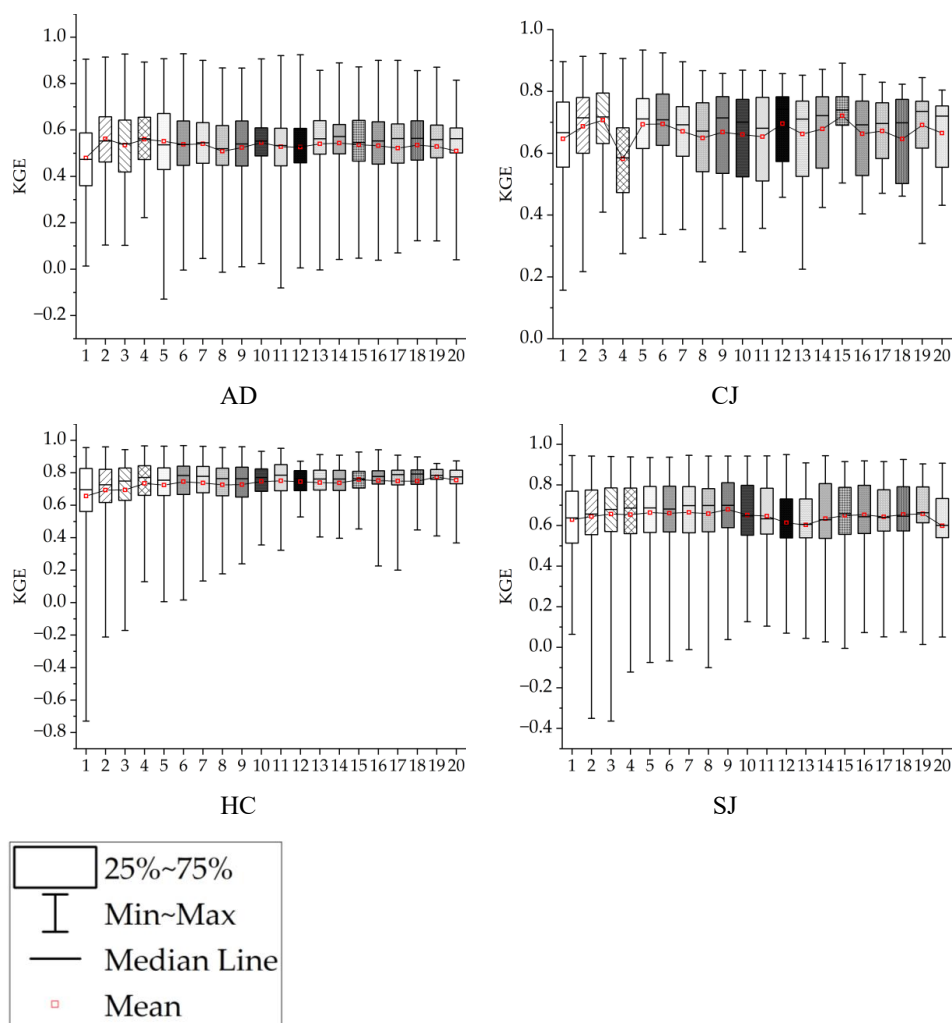


846 *Figure. 2. KGE values before and after calibration*

847



848



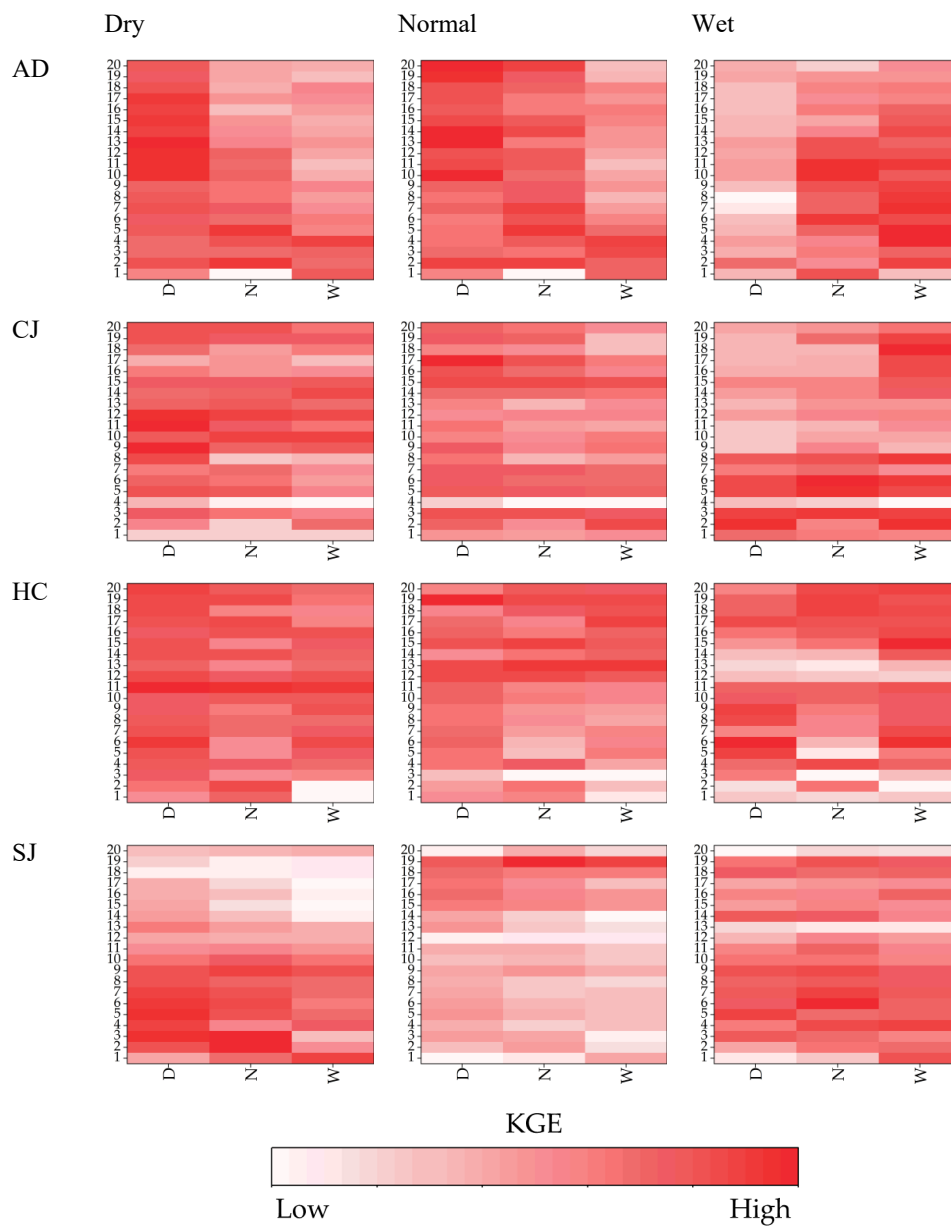
849 *Figure 3. Validation performances depending on data length of the calibration period*

850



851

Basins Hydrological conditions for validation period

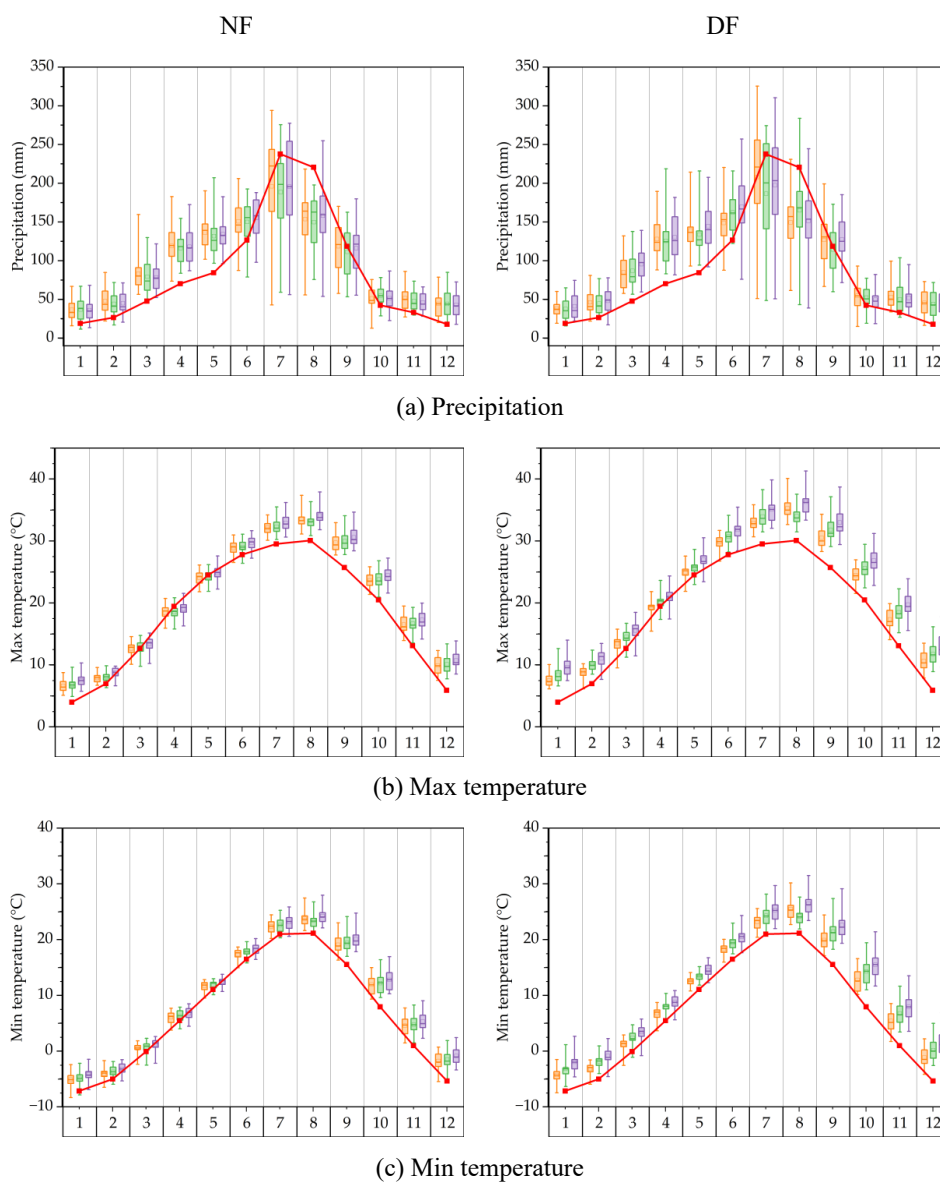


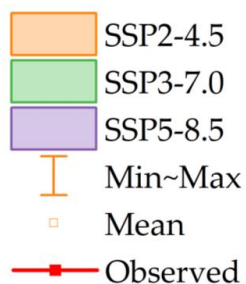
852 *Figure 4. KGEs classified by hydrological conditions for the calibration-validation period*

853



854





855

856 *Figure. 5. Projected annual changes in future precipitation (mm) and temperature (°C)*

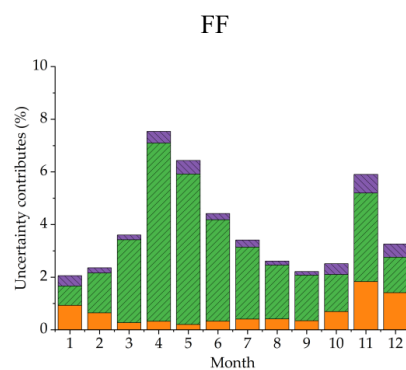
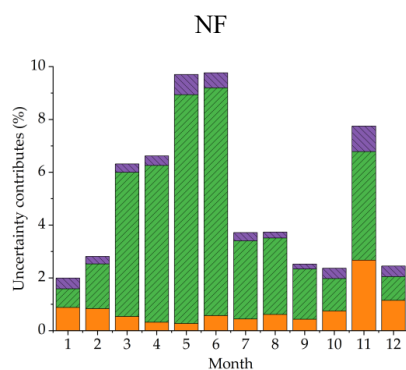
857



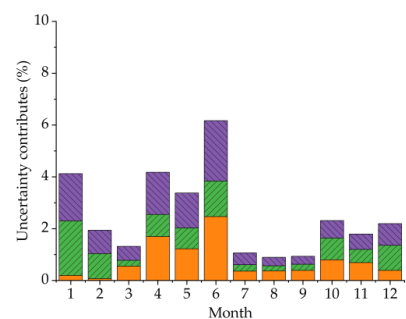
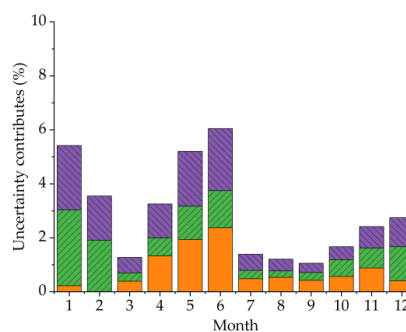
858

Basins

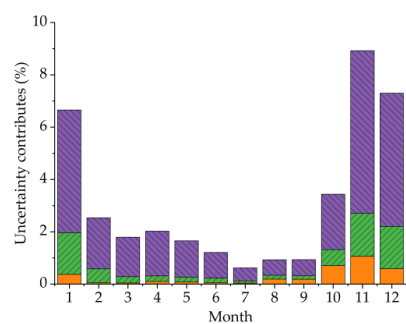
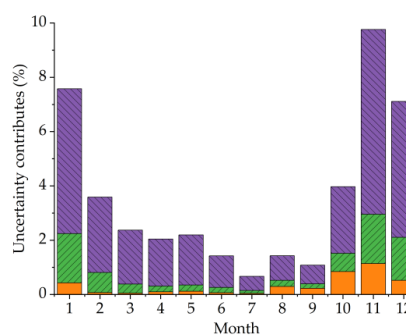
AD



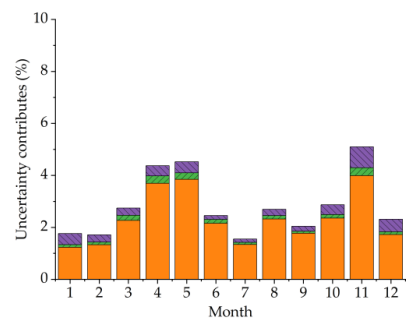
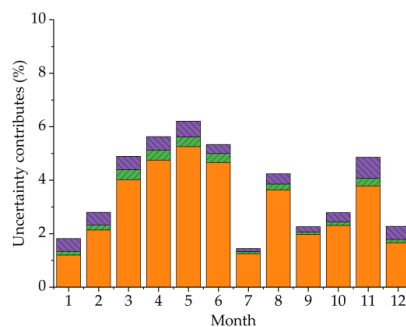
CJ

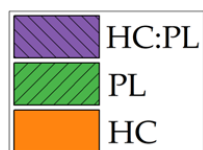


HC



SJ



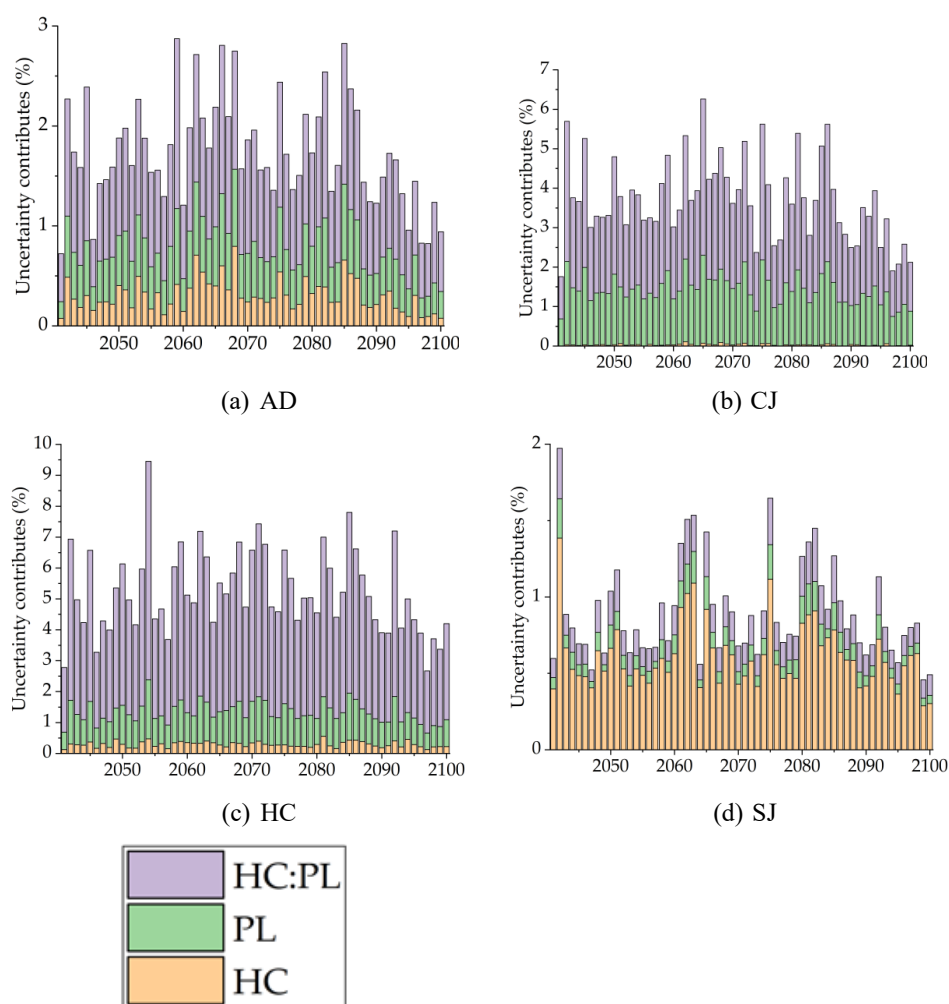


859 *Figure. 6. Contribution of hydrological model parameter to uncertainty in future runoff*
860 *projection using ANOVA*

861



862



863

864 *Figure 7. Contribution of hydrological model parameter to uncertainty in future*

865 *hydrological drought analysis*

866



867

868

Table 1. Validation performance according to hydrological conditions

Basins	Validation climatic conditions	Calibration period hydrological conditions		
		D	N	W
AD	D	0.480	0.401	0.382
	N	0.573	0.562	0.510
	W	0.571	0.621	0.642
CJ	D	0.743	0.727	0.725
	N	0.643	0.621	0.615
	W	0.674	0.686	0.706
HC	D	0.732	0.691	0.670
	N	0.738	0.719	0.714
	W	0.763	0.757	0.769
SJ	D	0.557	0.544	0.515
	N	0.677	0.671	0.650
	W	0.674	0.681	0.684

869

870



871 *Table 2. Changes from historical to future runoff for four dam basins*

872 (unit: %)

Basins	SSPs	NF				DF			
		Spring	Summer	Fall	Winter	Spring	Summer	Fall	Winter
AD	SSP2-4.5	82.1	-9.9	10.8	178.3	92.6	-5.3	18.1	179.2
	SS3-7.0	84.3	-11.1	6.7	168.3	104.3	-6.3	16.4	188.9
	SSP5-8.5	91.0	-5.7	12.9	194.2	118.9	1.2	26.7	216.1
CJ	SSP2-4.5	184.6	25.1	34.7	242.8	191.7	32.4	47.3	252.7
	SS3-7.0	186.6	21.0	32.8	226.7	210.2	27.6	44.7	276.5
	SSP5-8.5	148.8	8.0	0.8	173.1	157.2	14.0	13.1	192.0
HC	SSP2-4.5	207.6	2.7	-19.7	95.4	222.7	8.1	-12.3	100.8
	SS3-7.0	213.7	-1.3	-22.5	91.2	243.4	6.8	-12.7	109.0
	SSP5-8.5	223.2	5.7	-15.2	110.0	268.8	14.8	-3.3	127.4
SJ	SSP2-4.5	170.9	1.5	7.7	60.5	181.4	5.9	18.4	63.3
	SS3-7.0	175.1	-2.1	7.3	58.6	198.9	5.6	17.9	75.6
	SSP5-8.5	181.1	5.5	12.9	75.1	217.2	14.0	29.7	88.6

873

874



875 *Table 3. Differences in low runoff according to hydrological model parameters*

876 (unit: m³/s)

Basins	SSPs	NF		DF	
		Q ₇₅ Differ	Ratio (%)	Q ₇₅ Differ	Ratio (%)
AD	SSP2-4.5	7.24	10.28	7.00	10.42
	SSP3-7.0	7.04	9.58	7.71	9.56
	SSP5-8.5	7.43	9.32	7.88	9.94
CJ	SSP2-4.5	48.93	5.60	49.00	5.35
	SSP3-7.0	48.80	4.60	52.35	5.53
	SSP5-8.5	39.02	5.70	38.09	6.11
HC	SSP2-4.5	5.84	12.67	5.86	13.93
	SSP3-7.0	5.55	13.86	5.95	12.86
	SSP5-8.5	6.03	12.86	6.44	14.62
SJ	SSP2-4.5	4.61	9.84	4.51	9.61
	SSP3-7.0	4.23	11.24	4.64	9.76
	SSP5-8.5	4.64	9.37	4.97	9.12

877

878



879 *Table 4. Frequency of statistical significance ($p < 0.05$) of uncertainty sources for future*
880 *monthly runoff during the NF period*

Factor	Jan	Feb	Mar	Apr	May	Jun	Jul	Aug	Sep	Oct	Nov	Dec
GCM	4/4	4/4	4/4	4/4	4/4	4/4	4/4	4/4	4/4	4/4	4/4	4/4
SSP	4/4	4/4	4/4	4/4	4/4	4/4	4/4	4/4	4/4	4/4	4/4	4/4
HC	4/4	4/4	4/4	4/4	4/4	4/4	4/4	4/4	4/4	4/4	4/4	4/4
PL	4/4	4/4	4/4	4/4	4/4	4/4	4/4	4/4	4/4	4/4	4/4	4/4
GCM:SSP	4/4	4/4	4/4	4/4	4/4	4/4	4/4	4/4	4/4	4/4	4/4	4/4
GCM:HC	3/4	2/4	2/4	2/4	2/4	4/4	4/4	4/4	4/4	4/4	4/4	4/4
GCM:PL	4/4	4/4	4/4	4/4	4/4	4/4	4/4	4/4	4/4	4/4	4/4	4/4
SSP:HC	0/4	0/4	0/4	0/4	0/4	0/4	0/4	0/4	0/4	1/4	1/4	0/4
SSP:PL	0/4	0/4	0/4	0/4	0/4	1/4	2/4	1/4	0/4	1/4	0/4	0/4
HC:PL	4/4	4/4	4/4	4/4	4/4	4/4	4/4	4/4	4/4	4/4	4/4	4/4

881



882 *Table 5. Frequency of statistical significance ($p < 0.05$) of uncertainty sources for future*
 883 *monthly runoff during the DF period*

Factor	Jan	Feb	Mar	Apr	May	Jun	Jul	Aug	Sep	Oct	Nov	Dec
GCM	4/4	4/4	4/4	4/4	4/4	4/4	4/4	4/4	4/4	4/4	4/4	4/4
SSP	4/4	4/4	4/4	4/4	4/4	4/4	4/4	4/4	4/4	4/4	4/4	4/4
HC	4/4	4/4	4/4	4/4	4/4	4/4	4/4	4/4	4/4	4/4	4/4	4/4
PL	4/4	4/4	4/4	4/4	4/4	4/4	4/4	4/4	4/4	4/4	4/4	4/4
GCM:SSP	4/4	4/4	4/4	4/4	4/4	4/4	4/4	4/4	4/4	4/4	4/4	4/4
GCM:HC	4/4	4/4	4/4	4/4	4/4	4/4	4/4	4/4	4/4	4/4	4/4	4/4
GCM:PL	4/4	4/4	4/4	4/4	4/4	4/4	4/4	4/4	4/4	4/4	4/4	4/4
SSP:HC	0/4	0/4	0/4	0/4	0/4	0/4	0/4	0/4	0/4	0/4	0/4	0/4
SSP:PL	0/4	0/4	0/4	0/4	0/4	0/4	0/4	0/4	0/4	0/4	0/4	0/4
HC:PL	4/4	4/4	4/4	4/4	4/4	4/4	4/4	4/4	4/4	4/4	4/4	4/4

884



885 *Table 6. Differences in the number of drought events according to hydrological conditions*

886 (unit: occurrences)

SSPs	Basin	AD			CJ		
	Duration	3	6	12	3	6	12
245	NF	5.65	1.65	0.10	1.60	0.55	0.15
	DF	4.80	0.90	0.30	1.65	0.85	0.45
370	NF	6.25	1.65	0.45	1.60	0.20	0.55
	DF	4.35	0.90	0.25	1.85	0.55	0.30
585	NF	3.95	1.65	0.25	2.35	0.50	0.40
	DF	4.55	0.90	0.20	1.75	0.65	0.60
SSPs	Basin	HC			SJ		
	Duration	3	6	12	3	6	12
245	NF	0.40	0.25	0.10	1.45	0.60	0.15
	DF	0.45	1.25	0.85	2.00	0.30	0.10
370	NF	0.50	0.45	0.45	1.45	0.85	0.25
	DF	0.15	0.40	0.30	1.95	0.10	0.10
585	NF	0.55	0.20	0.15	2.50	0.30	0.35
	DF	0.45	0.30	0.50	1.65	0.35	0.30

887

888



889 *Table 7. Frequency of statistical significance ($p < 0.05$) of uncertainty sources for future*
890 *hydrological drought*

Factor	2040s	2050s	2060s	2070s	2080s	2090s
GCM	4/4	4/4	4/4	4/4	4/4	4/4
SSP	4/4	4/4	4/4	4/4	4/4	4/4
HC	4/4	4/4	4/4	4/4	4/4	4/4
PL	4/4	4/4	4/4	4/4	4/4	4/4
GCM:SSP	4/4	4/4	4/4	4/4	4/4	4/4
GCM:HC	4/4	4/4	4/4	4/4	4/4	4/4
GCM:PL	4/4	4/4	4/4	4/4	4/4	4/4
SSP:HC	0/4	0/4	0/4	0/4	0/4	0/4
SSP:PL	0/4	0/4	0/4	0/4	0/4	0/4
HC:PL	4/4	4/4	4/4	4/4	4/4	4/4

891



892 *Table 8. Uncertainty contribution in future hydrological drought analysis from hydrological*
893 *model calibration*

894 (unit: %)

Basins	NF	DF
AD	1.89	1.64
CJ	4.06	3.58
HC	5.56	5.27
SJ	0.26	0.26

895

896